Tuning Many-Body Interactions in Graphene: The Effects of Doping on Excitons and Carrier Lifetimes

Kin Fai Mak,[1] Felipe H. da Jornada,[2,3] Keliang He,[4] Jack Deslippe,[2,3,5] Nicholas Petrone,[6] James Hone,[6] Jie Shan,[4] Steven G. Louie,[2,3] and Tony F. Heinz[1,*]

[1]*Departments of Physics and Electrical Engineering, Columbia University, New York, New York 10027, USA*
[2]*Department of Physics, University of California, Berkeley, California 94720, USA*
[3]*Materials Sciences Division, Lawrence Berkeley National Laboratory, Berkeley, California 94720, USA*
[4]*Department of Physics, Case Western Reserve University, 10900 Euclid Avenue, Cleveland, Ohio 44106, USA*
[5]*National Energy Research Scientific Computing Center, Lawrence Berkeley National Laboratory, Berkeley, California 94720, USA*
[6]*Department of Mechanical Engineering, Columbia University, New York, New York 10027, USA*

(Received 26 December 2013; published 20 May 2014)

The optical properties of graphene are strongly affected by electron-electron (*e*-*e*) and electron-hole (*e*-*h*) interactions. Here we tune these many-body interactions through varying the density of free charge carriers. Measurements from the infrared to the ultraviolet reveal significant changes in the optical conductivity of graphene for both electron and hole doping. The shift, broadening, and modification in shape of the saddle-point exciton resonance reflect strong screening of the many-body interactions by the carriers, as well as changes in quasiparticle lifetimes. *Ab initio* calculations by the *GW* Bethe-Salpeter equation method, which take into account the modification of both the repulsive *e*-*e* and the attractive *e*-*h* interactions, provide excellent agreement with experiment. Understanding the optical properties and high-energy carrier dynamics of graphene over a wide range of doping is crucial for both fundamental graphene physics and for emerging applications of graphene in photonics.

DOI: 10.1103/PhysRevLett.112.207401 PACS numbers: 78.67.Wj, 73.22.Pr, 78.40.Ri, 78.66.Tr

Many of the distinctive properties of graphene, such as the characteristic linear dispersion relation of chiral massless Dirac fermions and the associated anomalous quantum Hall effect [1], can be understood within a picture of noninteracting electrons. These features are modified by many-body electronic interactions, leading to departures from the linear dispersion relation [2] and the presence of the fractional quantum Hall effect [3]. A similar situation prevails in terms of the optical response of graphene. The measured optical conductivity in the near infrared and visible is close to the value of $e^2/4\hbar$ expected within the single-particle theory [4,5]. Significant departures from the predictions of single-particle theory are, however, revealed in the optical spectrum of graphene in the ultraviolet (UV) [6–10]. There the saddle point in the Brillouin zone at the *M* point gives rise to a pronounced peak in the optical absorption. Both the position and shape of this feature reveal the role of strong Coulomb interactions, as predicted by theory [6]. Instead of simple band-to-band transitions, excitonic interactions give rise to resonances of correlated *e*-*h* pairs [6–13]. The same interactions also reduce the lifetime of high-energy quasiparticles [14–18].

Previous experimental investigations of excitonic effects in graphene have relied on line-shape analysis of the absorption spectrum of undoped graphene [7–9]. Direct control of many-body interactions through modification of carrier concentration provides a new vehicle to probe the pronounced excitonic effects. The ability to alter the excitonic interactions and the decay rate of quasiparticles by varying the dielectric screening of the Coulomb interactions is also important for the emerging area of graphene photonics [19]. In this Letter, we demonstrate strong tuning of many-body interactions in graphene by the free-carrier density. We probe these effects through their distinctive optical signature near the saddle-point resonance. The observed changes are completely unexpected from a picture of Pauli blocking of band-to-band transitions [4] and reveal the subtle effects of the different many-body interactions in this model 2D system. We are able to reproduce all significant aspects of the experimental results by *ab initio* excited-state calculations. In addition to the fundamental interest in the interactions of carriers in graphene, our findings show the possibility of modifying both the high-energy optical response of graphene and the decay processes of excited carriers. The latter suggests, for example, a means of tuning the Auger relaxation rates for more efficient carrier multiplication [20] and controlling the response time of saturable absorption in graphene.

In our study, we measured the optical sheet conductivity $\sigma(E)$ of graphene over a broad range of photon energies E from the near infrared to the UV ($1.2 \leq E \leq 5.5$ eV) for both electron and hole doping. Our experiments were performed using graphene field-effect transistors prepared on a transparent (quartz) substrate with a transparent electrolyte top gate [21,22]. We were able to examine the behavior at carrier concentrations exceeding 10^{14} cm^{-2}. The optical conductivity spectrum $\sigma(E)$ of the graphene layer was determined by absorption spectroscopy in the

transmission geometry. Accurate measurements of the influence of charge carriers were obtained by recording the differential response as a function of gating conditions.

The measured optical conductivity spectrum $\sigma(E)$ of graphene can be seen to display marked changes as a function of carrier concentration [Fig. 1(a)]. At low photon energies, we observe a progressive suppression of optical absorption with increasing doping. In addition, the peak in $\sigma(E)$ observed in the UV around 4.6 eV is found to be strongly influenced by the carrier density. The changes in $\sigma(E)$ at low photon energies can be explained within the single-particle picture as the result of state filling, i.e., Pauli blocking of the interband transitions. The same does not apply to the doping-induced changes in the UV response, since there is no modification of the occupation of the states involved in the optical transitions at the relevant doping levels. The UV response, associated with the saddle-point exciton resonance at the M point of the graphene Brillouin zone [6–10], thus provides a direct signature of many-body interactions in graphene and of how carrier screening modifies these interactions.

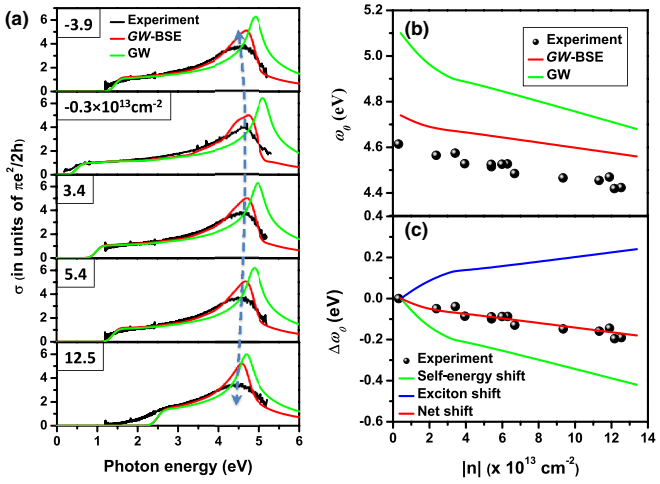

FIG. 1 (color online). Optical response of graphene as a function of doping, showing results of experiment (black line or symbols), of GW calculations (green line), and of GW-BSE calculations (red line). (a) The optical conductivity $\sigma(E)$ of graphene as a function of photon energy E for different doping densities n. A redshift of the experimentally observed peak in the UV is observed for both electron and hole doping. The position of the peak and its variation with doping are captured by GW-BSE calculations. The GW calculations, which omit e-h interactions, overestimate the resonance energy for all doping densities. (b) The resonance energy ω_0 as a function of doping density, with combined data for electron and hole doping. (c) The shift $\Delta\omega_0$ in resonance energy from that at charge neutrality as a function of doping, with combined data for electron and hole doping. The net shift (red line) calculated within the GW-BSE method is decomposed into two opposing contributions from screening of the electron self-energy (green line) and of the excitonic response (blue line). Effects due to finite lifetime of the excited electron and hole have not been included in the GW and GW-BSE calculations for the theoretical curves in this figure.

We note two important trends in the UV response. For increased doping by either electrons or holes, (i) the peak of the saddle-point exciton resonance energy ω_0 redshifts, and (ii) the peak feature becomes more symmetrical and broadens in width. The resonance energy ω_0 shifts from 4.62 eV at charge neutrality to 4.42 eV at high doping levels [Fig. 1(b)] [27], corresponding to an energy shift $\Delta\omega_0$ as large as 200 meV [Fig. 1(c)]. In addition, to experimental accuracy, we did not observe any increase in absorbance in the visible region from doping, aside from the effect of Pauli blocking noted above.

To understand the experimental results, we need to examine the different many-body effects in graphene and how the increased carrier screening in the doped samples modifies these interactions. The observed changes in both the position and asymmetry of the saddle-point exciton feature with doping can be explained on this basis. The emergence of a more symmetrical absorption feature with increased doping level reflects the reduced strength of e-h interactions due to enhanced carrier screening, since a symmetrical line shape is expected for band-to-band transitions at a 2D saddle-point singularity in the joint density of states [28]. The redshift in the peak position of the saddle-point exciton requires consideration of screening of both the attractive e-h interactions and the repulsive e-e interactions, with the repulsive term dominating over the attractive one. The data also reveal an increased width of the saddle-point exciton resonance with increasing doping. This effect suggests a decreased lifetime of the optically excited states arising from decay of the optically excited carriers by scattering with the additional carriers near the Fermi surface. We have been able to substantiate all elements of this heuristic picture by rigorous *ab initio* many-body theory, as well as to reproduce accurately the experimental absorption spectrum and its variation with doping level without the introduction of any adjustable parameters.

The theoretical approach is based on *ab initio* GW [29] and GW–Bethe-Salpeter equation (GW-BSE) calculations [30,31] of the conductivity spectra at different doping levels [Fig. 1(a)], which were performed using the BerkeleyGW package [22,32]. The levels of carrier doping in graphene reached in our study are quite high, so the intrinsic screening due to electrons in the doped graphene should dominate over other screening processes. Accordingly, we have explicitly calculated the doping-dependent dielectric matrix of freestanding graphene, while neglecting the substrate screening. The absorption spectra calculated within the GW approximation (which do not include e-h interactions) display a saddle-point resonance that is significantly blueshifted from the experimental spectra. Moreover, the predicted redshift in this resonance with increasing doping is far stronger than that observed experimentally [Figs. 1(a)–1(c)]. On the other hand, when excitonic effects are included in the full GW-BSE calculations, the theory reproduces the experimental results quite

accurately. The doping dependence of the peak position ω_0 [Fig. 1(b)] and, particularly, of the peak shift $\Delta\omega_0$ [Fig. 1(c)] is in excellent agreement with experiment.

To understand the physics behind the shift $\Delta\omega_0$ of the saddle-point exciton energy with doping, we decompose this quantity into two contributions [Fig. 1(c)]: (i) the change in the renormalization of quasiparticle self-energy and (ii) the change in the excitonic correction to the spectrum. Both effects can be explained in terms of the influence of carrier screening. This increased screening with increasing doping level reduces the energy needed for quasiparticles with a given momentum to be created, leading to the redshift associated with the first contribution. The enhanced screening also reduces the attractive *e*-*h* interactions. This reduces the original redshift from excitonic interactions in the neutral case. The excitonic contribution offsets about half of the redshift from decreased spacing of quasiparticle bands. The net result is a redshift of the saddle-point resonance $\Delta\omega_0$ with increasing doping that explains the experimental data quantitatively [Fig. 1(c)].

Although the *GW*-BSE calculations at this stage correctly capture the experimental peak shift with doping, the shape of the conductivity spectra calculated without lifetime effects of the quasiparticles significantly deviates from the observed spectral line shape [Fig. 1(a)]. More specifically, the experimental excitonic features are all broader than those predicted by the calculations. While the calculations display sharper excitonic features at high doping levels than at low doping levels, the opposite trend is seen experimentally. We address this issue by including an *ab initio* calculation of the excited-state lifetimes as a function of doping.

To determine the exciton line shape, we consider separately the decay (i.e., the imaginary part of the self-energy) of quasielectrons and quasiholes produced by optical excitation. We then derive the many-body contributions to the exciton linewidth (i.e., going beyond the independent particle picture) by including the imaginary part of the quasiparticle energies perturbatively in the Bethe-Salpeter equation in a similar way as in Ref. [33]. This approach results in the following expression:

$$(\tau^S)^{-1} = \sum_{vc\mathbf{k}} |A^S_{vc\mathbf{k}}|^2 (\tau^{-1}_{c\mathbf{k}} + \tau^{-1}_{v\mathbf{k}}),$$

where $(\tau^S)^{-1}$ is the broadening associated with the solution $|S\rangle$ to the Bethe-Salpeter equation, $\tau_{n\mathbf{k}}$ is the quasiparticle lifetime for band n and wave vector $\mathbf{k}$, and $A^S_{vc\mathbf{k}}$ is the coefficient that defines $|S\rangle$ in terms of an expansion in free quasielectron and quasihole excitations $|S\rangle = \sum_{vc\mathbf{k}} A^S_{vc\mathbf{k}} |c,\mathbf{k}\rangle \otimes |v,\mathbf{k}\rangle$.

The quasiparticle lifetime is directly related to the imaginary part of the self-energy through $\mathrm{Im}\Sigma_{n\mathbf{k}}(\epsilon_{n\mathbf{k}},\omega) = \tau^{-1}_{n\mathbf{k}}$, where $\epsilon_{n\mathbf{k}}$ is the quasiparticle energy. The self-energy has contributions from *e*-*e* and electron-phonon (*e*-ph) interactions. We calculated the lifetimes arising from *e*-*e* interactions for four different doping levels and also included the effect of *e*-ph interactions from our previous study [18].

The optical conductivity of graphene calculated including quasiparticle lifetime effects in the *GW*-BSE calculations is in excellent agreement with experiment for both neutral and doped graphene (Fig. 2). The complete theory not only replicates the absolute exciton energy and the shift in energy with doping, as before, but also captures the change in width of the saddle-point exciton and its evolution to a more symmetric shape with increased doping. The agreement, we note, is obtained using a theory that contains no adjustable parameters.

It is instructive to compare the *ab initio* theoretical predictions for the linewidth of the saddle-point exciton with the experimental broadening (Fig. 3). As expected from the agreement of the conductivity spectra, the experimental widths agree well with theory, both in magnitude and in their variation with doping density. For the case of theory, we further identify contributions to the broadening arising from *e*-ph and *e*-*e* interactions, respectively [22].

The contribution to the exciton line width arising from *e*-ph interactions is seen to remain nearly constant as a function of doping. This behavior reflects the fact that near the saddle point, the imaginary part of the quasiparticle self-energy due to *e*-ph interactions, while varying with the quasiparticle energy, has little dependence on the doping level [18]. In contrast, the interactions of the highly excited quasiparticles with other electrons, i.e., the *e*-*e* interactions,

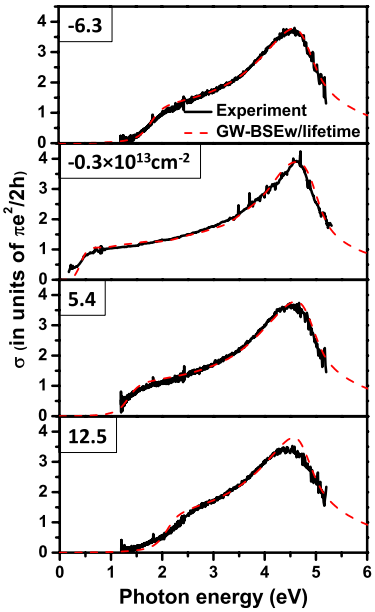

FIG. 2 (color online). *Ab initio* calculations of the optical conductivity spectra $\sigma(E)$ including lifetime effects. The calculated *GW*-BSE conductivity spectra with quasiparticle lifetime effects included (red dashed lines) are compared to the experimental spectra (black lines) for four different doping densities. By evaluating the influence of both *e*-*e* and *e*-ph decay channels for the optically excited states, we obtain agreement with the experimental spectra for all doping levels.

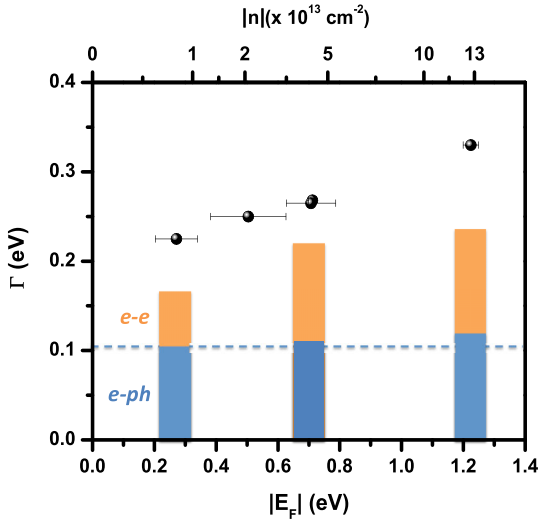

FIG. 3 (color online). Decay rates of highly excited quasiparticles in graphene. The linewidth of the saddle-point exciton (as discussed in the text) is shown as a function of absolute doping level (for doping densities shown in Fig. 2), given in terms of the Fermi energy, for measurements with both electron and hole doping. The dots are the experimental values, while the columns show the calculated contributions from *e*-ph (blue) and *e*-*e* (orange) interactions. The horizontal dotted line is a guide to the eye.

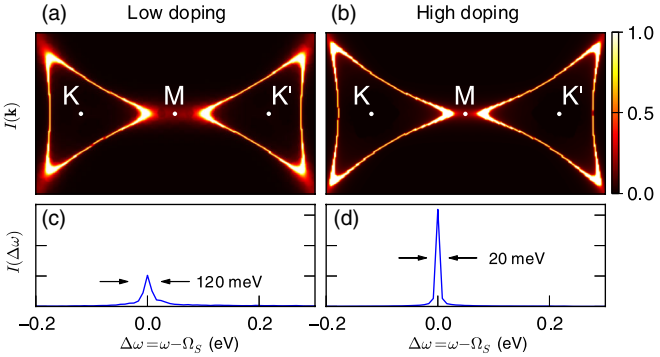

FIG. 4 (color online). Calculated redistribution of oscillator strength. The *k*-space distribution of the oscillator strength $I(\mathbf{k})$ is plotted for (a) a low carrier doping density ($n = 0.4\times 10^{13}$ cm^{-2}) and (b) a high doping density ($n = 13\times 10^{13}$ cm^{-2}). The corresponding energy distribution of oscillator strength $I(\Delta\omega)$ is also shown for (c) the low and (d) the high doping levels.

increase with doping. We attribute this increase to the enlargement of the Fermi surface with doping, which increases the number of available decay channels for the quasiparticles [16,18]. For these highly excited quasiparticles, the decay from *e*-*e* interactions is not negligible even at low doping levels. We note that the decay process is influenced by the detailed band structure of graphene; the self-energy of quasiparticles for states near the saddle point is quite anisotropic and the broadening of the saddle-point resonance arises largely from the rapid decay of states in the $K \rightarrow \Gamma$ direction.

In addition to the changes in the quasiparticle decay rates, the linewidth of the optical absorption near the saddle-point resonance is also influenced by the range of free *e*-*h* pairs that participate in absorption at a specific photon energy [6]. This can be quantified by defining a *k*-space distribution of the oscillator strength from a narrow energy window of exciton states, $I(\mathbf{k}) = \sum_S |A^S_{\mathbf{k}} \langle v\mathbf{k}|\mathbf{v}\cdot\hat{\mathbf{e}}|c\mathbf{k}\rangle|$ [Figs. 4(a) and 4(b)], where $A^S_{\mathbf{k}}$ is the coefficient of expansion of the exciton eigenstate in terms of the free quasiparticle states $|c\mathbf{k}\rangle$ and $\langle v\mathbf{k}|$, $\langle v\mathbf{k}|\mathbf{v}\cdot\hat{\mathbf{e}}|c\mathbf{k}\rangle$ is the independent particle optical transition matrix element, and the summation is over states S with energies Ω_S within a window of ± 75 meV at the peak position. A similar distribution can be defined as a function of the quasiparticles' energies as $I(\Delta\omega) = \sum_{S,\mathbf{k}} |A^S_{\mathbf{k}} \langle v\mathbf{k}|\mathbf{v}\cdot\hat{\mathbf{e}}|c\mathbf{k}\rangle| \delta[\Delta\omega - (\epsilon_{c\mathbf{k}} - \epsilon_{v\mathbf{k}} - \Omega_S)]$ [Figs. 4(c) and 4(d)]. Upon increasing doping, both the *k*-space [Fig. 4(b)] and energy [Fig. 4(d)] distributions become more localized, which shows that there is less redistribution of oscillator strength among different regions of the band structure when the *e*-*h* interactions are screened. In fact, in the highly doped samples, the oscillator strength associated with the peak of the conductivity spectrum mainly comes from regions near the *M* point, which explains why the *GW*-BSE conductivity spectra approach the *GW* ones for highly doped samples.

The decrease in the number of participating *e*-*h* pair configurations upon doping is also important for the fine details of the linewidth of the saddle-point exciton. While the scattering rate of a state at a particular momentum tends to increase with doping, the reduction in the *e*-*h* correlation effects causes the overall linewidth of the exciton resonance to show a weak saturation in our theory (Fig. 3). The higher experimental values may be attributed to the influence of inhomogeneity in the doping level of the sample in experiment, as well as approximations in the theory from the omission of dynamical screening effects in the *e*-*h* interaction kernel [34] and substrate interactions [35].

In conclusion, our combined experimental and theoretical investigation has provided a coherent understanding of the nature of optical transitions in graphene and of the manner in which tuning the many-body interactions through doping alters the graphene optical conductivity spectrum. This knowledge is not only of fundamental importance, but also has significant implications for the rapidly developing areas of graphene photonics and optoelectronics.

We acknowledge helpful discussions with Dr. Mark Hybertsen. Support for the growth of the graphene samples was provided by the U.S. Department of Energy (DOE) through the Energy Frontier Research Center at Columbia University (Grant No. DESC00001085). Device fabrication was supported by the U.S. Office of Naval Research (ONR) at Columbia University and by the National Science Foundation (NSF Grant No. DMR-0907477) at Case

Western Reserve University. Optical characterization and analysis was supported by the NSF (Grant No. DMR-1106225). The theoretical formulation and study of lifetime effects was supported by the NSF (Grant No. DMR10-1006184) and by the ONR under the MURI program at University of California, Berkeley. This research is also supported by the Theory Program (simulation and analysis of the optical absorption) and the SciDAC Program on Excited State Phenomena in Energy Materials (algorithms and code developments) funded by the U.S. Department of Energy, the Office of Basic Energy Sciences and of Advanced Scientific Computing Research, under Contract No. DE-AC02-05CH11231 at the Lawrence Berkeley National Laboratory. S. G. L. acknowledges support of a Simons Foundation Fellowship in Theoretical Physics. Computational resources were provided by the DOE at Lawrence Berkeley National Laboratory's NERSC facility. K. F. M. and F. H. J. contributed equally to this work.

*Corresponding author.
tony.heinz@columbia.edu

[1] K. S. Novoselov, A. K. Geim, S. V. Morozov, D. Jiang, M. I. Katsnelson, I. V. Grigorieva, S. V. Dubonos, and A. A. Firsov, Nature (London) **438**, 197 (2005); Y. B. Zhang, Y. W. Tan, H. L. Stormer, and P. Kim, Nature (London) **438**, 201 (2005).
[2] D. C. Elias *et al.*, Nat. Phys. **7**, 701 (2011).
[3] K. I. Bolotin, F. Ghahari, M. D. Shulman, H. L. Stormer, and P. Kim, Nature (London) **462**, 196 (2009); X. Du, I. Skachko, F. Duerr, A. Luican, and E. Y. Andrei, Nature (London) **462**, 192 (2009).
[4] R. R. Nair, P. Blake, A. N. Grigorenko, K. S. Novoselov, T. J. Booth, T. Stauber, N. M. R. Peres, and A. K. Geim, Science **320**, 1308 (2008); K. F. Mak, M. Y. Sfeir, Y. Wu, C. H. Lui, J. A. Misewich, and T. F. Heinz, Phys. Rev. Lett. **101**, 196405 (2008); Z. Q. Li, E. A. Henriksen, Z. Jiang, Z. Hao, M. C. Martin, P. Kim, H. L. Stormer, and D. N. Basov, Nat. Phys. **4**, 532 (2008); A. B. Kuzmenko, E. van Heumen, F. Carbone, and D. van der Marel, Phys. Rev. Lett. **100**, 117401 (2008); F. Wang, Y. Zhang, C. Tian, C. Girit, A. Zettl, M. Crommie, and Y. R. Shen, Science **320**, 206 (2008).
[5] T. Ando, Y. Zheng, and H. Suzuura, J. Phys. Soc. Jpn. **71**, 1318 (2002); V. P. Gusynin, S. G. Sharapov, and J. P. Carbotte, Phys. Rev. Lett. **96**, 256802 (2006); N. M. R. Peres, F. Guinea, and A. H. Castro Neto, Phys. Rev. B **73**, 125411 (2006); D. S. L. Abergel and V. I. Fal'ko, Phys. Rev. B **75**, 155430 (2007); T. Stauber, N. M. R. Peres, and A. K. Geim, Phys. Rev. B **78**, 085432 (2008).
[6] L. Yang, J. Deslippe, C.-H. Park, M. L. Cohen, and S. G. Louie, Phys. Rev. Lett. **103**, 186802 (2009).
[7] V. G. Kravets, A. N. Grigorenko, R. R. Nair, P. Blake, S. Anissimova, K. S. Novoselov, and A. K. Geim, Phys. Rev. B **81**, 155413 (2010).
[8] K. F. Mak, J. Shan, and T. F. Heinz, Phys. Rev. Lett. **106**, 046401 (2011).
[9] D.-H. Chae, Tobias Utikal, S. Weisenburger, H. Giessen, K. v. Klitzing, M. Lippitz, and J. Smet, Nano Lett. **11**, 1379 (2011).
[10] L. Yang, Nano Lett. **11**, 3844 (2011).
[11] E. G. Mishchenko, Phys. Rev. Lett. **98**, 216801 (2007).
[12] N. M. R. Peres, R. M. Ribeiro, and A. H. Castro Neto, Phys. Rev. Lett. **105**, 055501 (2010).
[13] S. H. Abedinpour, G. Vignale, A. Principi, M. Polini, W.-K. Tse, and A. H. MacDonald, Phys. Rev. B **84**, 045429 (2011).
[14] A. Bostwick, T. Ohta, T. Seyller, K. Horn, and E. Rotenberg, Nat. Phys. **3**, 36 (2007).
[15] D. A. Siegel, C.-H. Park, C. Hwang, J. Deslippe, A. V. Fedorov, S. G. Louie, and A. Lanzara, Proc. Natl. Acad. Sci. U.S.A. **108**, 11365 (2011).
[16] E. H. Hwang, Ben Yu-Kuang Hu, and S. Das Sarma, Phys. Rev. B **76**, 115434 (2007).
[17] M. Polini, R. Asgari, G. Borghi, Y. Barlas, T. Pereg-Barnea, and A. MacDonald, Phys. Rev. B **77**, 081411 (2008).
[18] C.-H. Park, F. Giustino, C. D. Spataru, M. L. Cohen, and S. G. Louie, Phys. Rev. Lett. **102**, 076803 (2009).
[19] F. Bonaccorso, Z. Sun, T. Hasan, and A. C. Ferrari, Nat. Photonics **4**, 611 (2010).
[20] T. Winzer, A. Knorr, and E. Malic, Nano Lett. **10**, 4839 (2010); J. C. W. Song, K. J. Tielrooij, F. H. L. Koppens, and L. S. Levitov, Phys. Rev. B **87**, 155429 (2013).
[21] K. F. Mak, C. H. Lui, J. Shan, and T. F. Heinz, Phys. Rev. Lett. **102**, 256405 (2009); D. K. Efetov and P. Kim, Phys. Rev. Lett. **105**, 256805 (2010).
[22] See Supplemental Material at http://link.aps.org/supplemental/10.1103/PhysRevLett.112.207401, which includes Refs. [4, 8, 21, 23–26, 29, 30, 32].
[23] X. S. Li *et al.*, Science **324**, 1312 (2009).
[24] M. S. Hybertsen and S. G. Louie, Phys. Rev. Lett. **55**, 1418 (1985).
[25] R. Kitamura, L. Pilon, and M. Jonasz, Appl. Opt. **46**, 8118 (2007).
[26] R. M. A. Azzam and N. M. Bashara, *Ellipsometry and Polarized Light* (North-Holland, Amsterdam, 1977).
[27] Because of Pauli blocking, interband optical transitions in graphene are suppressed at photon energies E below twice the Fermi level E_F . For a given gate voltage V, we determined the graphene Fermi energy as half of the photon energy $E_0(V)$ at which the optical conductivity in the visible range had the steepest slope . We then obtained the sheet carrier density n as a function of E_F, and, hence, of gate voltage V, using our *ab initio* calculations of the quasiparticle band structure (Fig. S1b of the Supplemental Material [22]). These calculations include the effects of screening of the quasiparticle self-energy, as reflected in a renormalized Fermi velocity.
[28] F. Bassani and G. Pastori Parravicini, *Electronic States and Optical Transitions in Solids* (Pergamon Press, New York, 1975).
[29] M. S. Hybertsen and S. G. Louie, Phys. Rev. B **34**, 5390 (1986).
[30] M. Rohlfing and S. G. Louie, Phys. Rev. Lett. **80**, 3320 (1998).
[31] S. Albrecht, L. Reining, R. Del Sole, and G. Onida, Phys. Rev. Lett. **80**, 4510 (1998); L. X. Benedict, E. L. Shirley, and R. B. Bohn, Phys. Rev. Lett. **80**, 4514 (1998).
[32] J. Deslippe *et al.*, Comput. Phys. Commun. **133**, 1269 (2011).
[33] A. Marini, Phys. Rev. Lett. **101**, 106405 (2008).
[34] M. Rohlfing and S. G. Louie, Phys. Rev. B **62**, 4927 (2000).
[35] T. Stauber, N. M. R. Peres, and A. H. Castro Neto, Phys. Rev. B **78**, 085418 (2008).